

Expanded View Figures

Figure EV1. SFRP1 enhances glial cell activation.

- A On the left, diagram of the observed GFP distribution (green dots) after lentiviral (LV) particles' delivery into the lateral ventricle (Lv). The dashed boxes represent areas shown in (B) and (D), 1 points to the wall of the lateral ventricle, and 2 to the Rostral Migratory Stream. Images on the right show examples of immunostaining against GFP protein (GFP signal was no longer visible, unless detected with immunohistochemistry) in the Lv of brains transduced with LV-*IRES-Gfp* or LV-*Sfrp1-IRES-Gfp* 5 months (m) post-infusion. Scale bar: 100 μ m.
- B Double immunostaining against GFP (green) and GFAP (magenta) of brains transduced with LV-*Sfrp1-IRES-Gfp*, indicating that transduced cells include astrocytes. Arrowheads indicate GFP⁺ astrocytes. Scale bar: 50 μ m.
- C The graphs show the number of Sox9 immunopositive cells, S100 β and Cleac7a immune intensity level and CD45 immunopositive area in LV-*Sfrp1-IRES-Gfp*-infected brains normalized against the mean value obtained in LV-*IRES-Gfp*-infected control brains. Dots represent the mean value obtained by the analysis of 6 sections for each biological replica ($n = 4-6$, mice per group). Error bars represent standard error. Statistical significance: * $P < 0.05$; ** $P < 0.01$ by two-sided Student's t -test.
- D Coronal sections from LV-*IRES-Gfp*- or LV-*Sfrp1-IRES-Gfp*-infected brains 1 or 5 months (m) post-infusion (PI). Sections were immunostained for CD45. Arrowheads indicate CD45^{hi}-positive macrophages or lymphocytes infiltrated in the parenchyma after prolonged LV-*Sfrp1-IRES-Gfp* infection. High-power images 1 and 2 were taken from the regions indicated with grey dotted lines in A. Scale bar: 50 μ m.
- E Coronal sections from wt and *Sfrp1*^{-/-} mouse brains three days after infusion of saline or LPS, immunostained for GFAP. The white arrows indicate the injection site; the area boxed with white lines is represented at high power in Fig 2. Scale bar: 100 μ m.

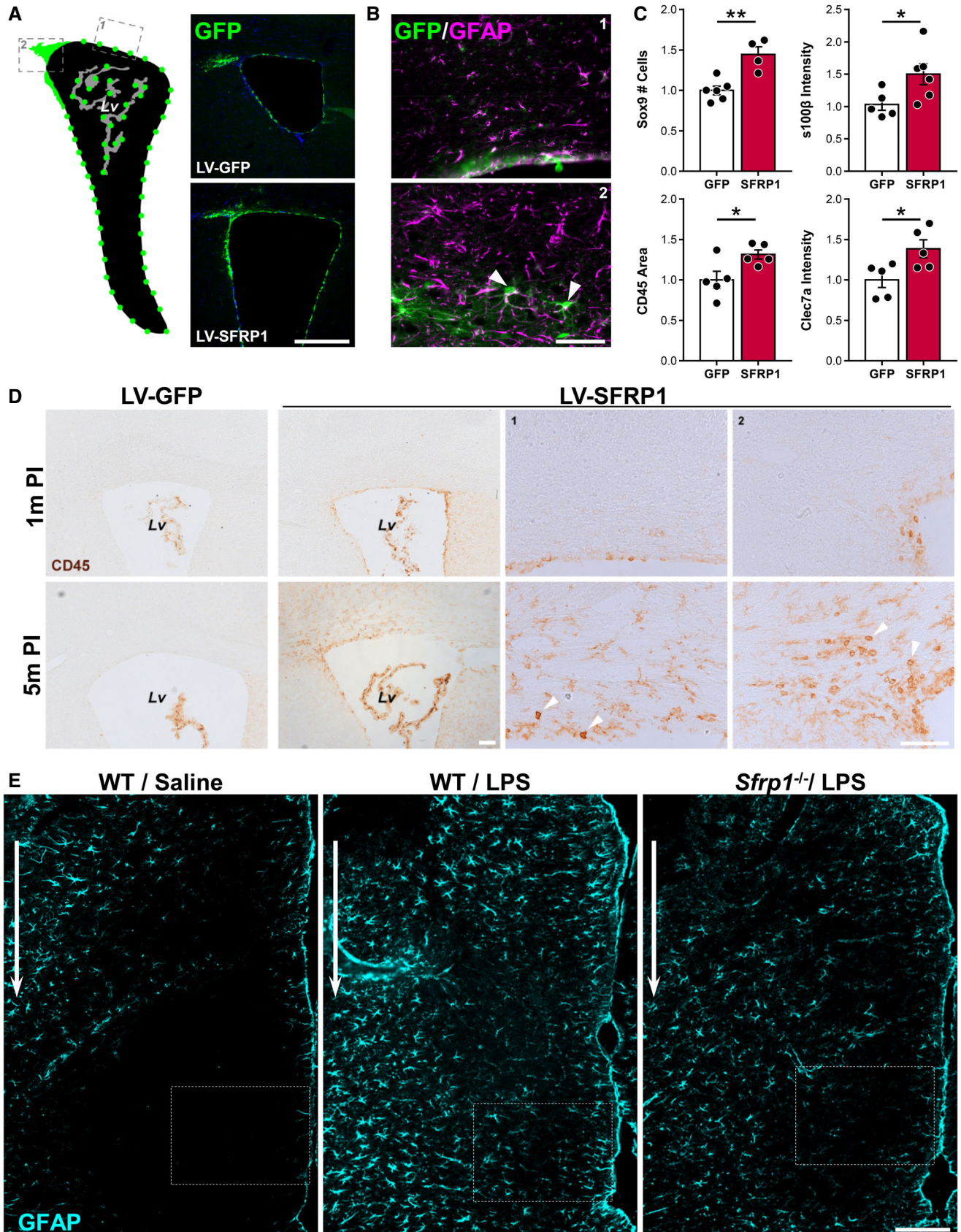


Figure EV1.

Figure EV2. SFRP1 enhances microglial cell activation and phagocytosis.

- A The graph shows the % of CD11b⁺ populations present in the cortex of *CX₃CR1^{GFP/+}* or *CX₃CR1^{GFP/+};Sfrp1^{-/-}* mice 3 days after saline or LPS intraventricular infusion (*n* = 5 per genotype and condition). Gating was set for isolating the following myeloid cell populations: CD11b⁺; CD45^{lo}; GFP⁺ surveying microglia, CD11b⁺; CD45⁺; GFP⁺ activated microglia and CD11b⁺; CD45⁺; GFP⁺ infiltrated monocytes. Error bars represent standard error.
- B The graph shows the pHrodo mean fluorescent signal present in GFP/CD45^{hi} and GFP/CD45^{low} cell populations isolated from cortex of *CX₃CR1^{GFP/+}* or *CX₃CR1^{GFP/+}; Sfrp1^{-/-}* mice 3 days after pHrodo intraventricular infusion (*n* = 4/5 per genotype respectively). Error bars represent standard error. Statistical significance: ***P* < 0.01 by two-way ANOVA followed by Bonferroni's multiple comparisons test.
- C Representative cytometric plots of brain cells suspension showing gating of individualized live cells CD11b⁺; CX3CR1⁺ recognized as microglial cells for pHrodo-labelled *E. coli* BioParticles quantitation. Comparison of microglial cells exposed (GFP⁺; CD45^{lo} and GFP⁺; CD45⁺ or not exposed (Ctrl-) to pHrodo-labelled *E. coli* shows specific pHrodo recognition.
- D Representative confocal image of FACS-sorted GFP⁺ microglia. Note specific pHrodo⁺ lysosomal inclusion of *E.coli* particles in phagocytosing vs non-phagocytosing microglia. Scale bar: 5µm.
- E The graphs show the quantification of the normalized total fluorescence from phagocytized pHrodo-labelled *E. coli* BioParticles and percentage of CD11b⁺ phagocytosing cells in the presence of wt or *Sfrp1^{-/-}* astrocytes (*n* = 4 cultures per condition). Error bars represent standard error. Statistical significance: Student's *t*-test.

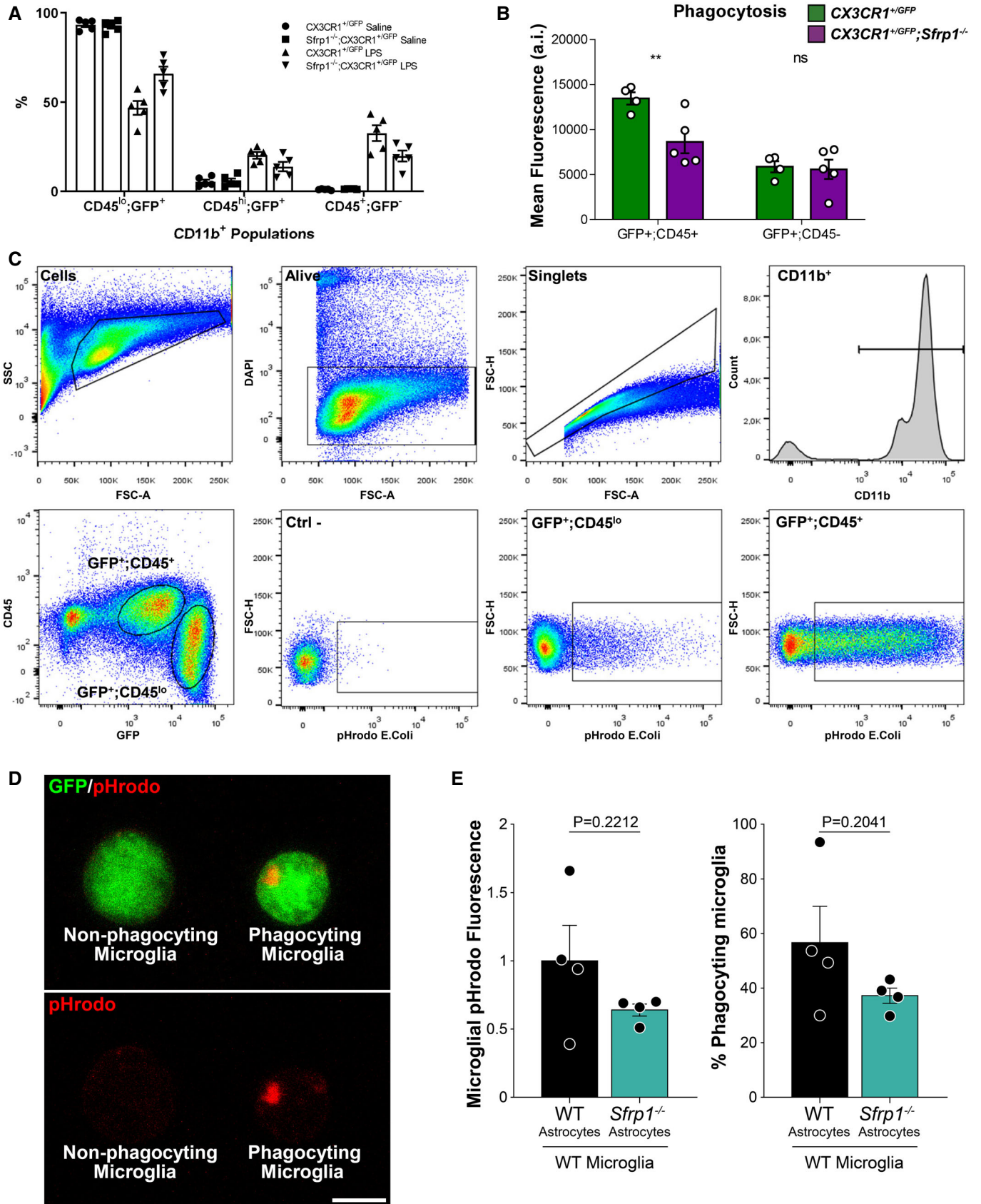


Figure EV2.

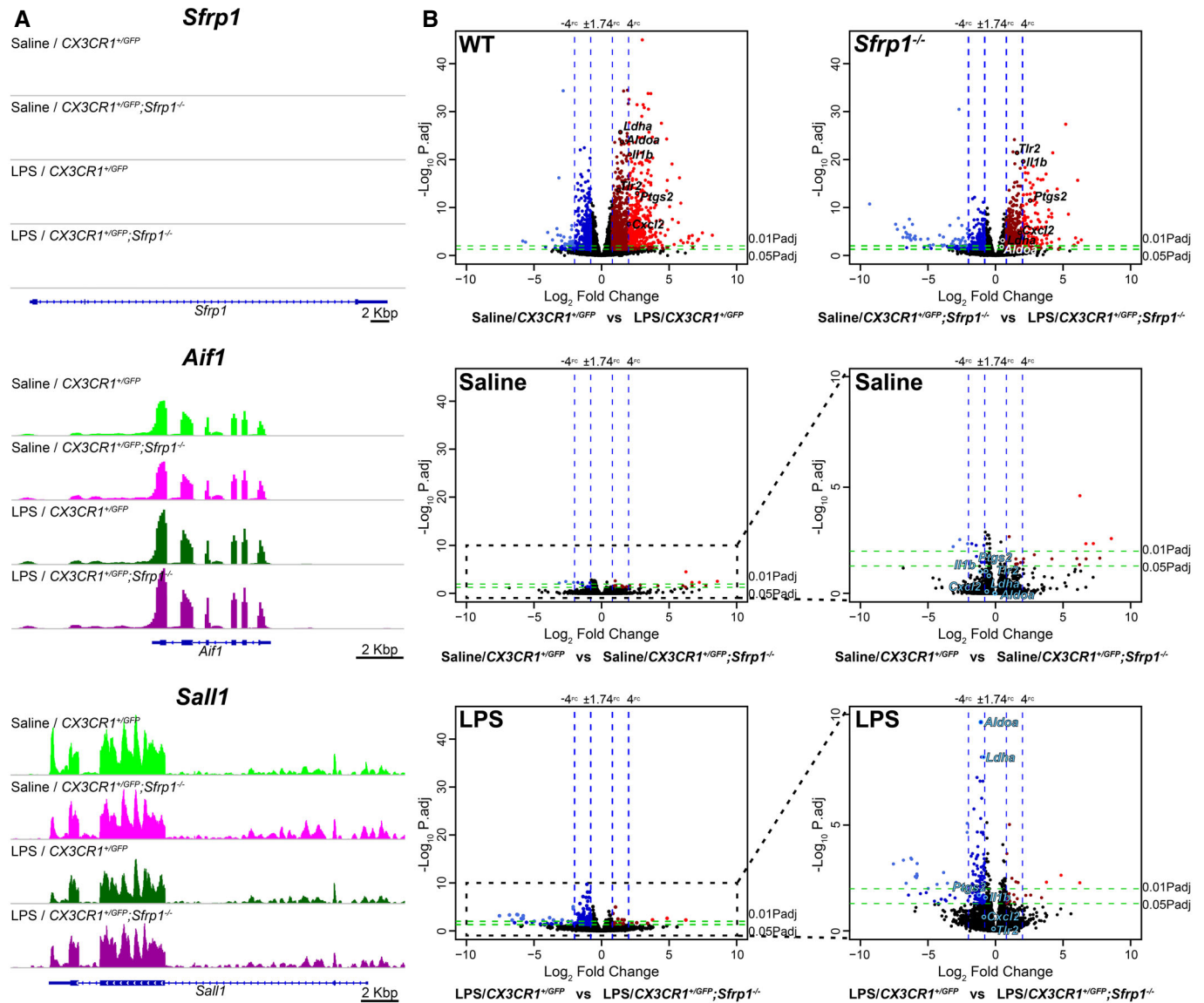


Figure EV3. Non-cell-autonomous effect of *Sfrp1* on microglial response to LPS.

A Integrative Genomics Viewer transcription profile of *Sfrp1* and the microglial specific genes *Aif1* and *Sall1* in microglial cells isolated from saline and LPS treatment of *CX₃CR1^{GFP/+}* and *CX₃CR1^{GFP/+};Sfrp1^{-/-}* mice. Scale bar: 2 Kbp.

B Volcano plots of differential gene expression from *CX₃CR1^{GFP/+}* or *CX₃CR1^{GFP/+};Sfrp1^{-/-}* microglial cell in response to saline or LPS. Data are represented as log₂ fold change vs -Log₁₀ adjusted *P*-value by the Wald test corrected for multiple comparisons by the Benjamini and Hochberg method. Note that expression variations associated with genotype in saline-treated animals are minimal. The effect of the genotype is evident only after LPS treatment. Genes with an expression change higher than 75% and an adjusted *P*-value < 0.05 are highlighted in dark red (+FC) and dark blue (-FC). Genes with an expression change higher than 400% and an adjusted *P*-value < 0.01 are highlighted in light red (+FC) and light blue (-FC).

Figure EV4. SFRP1 microglial inflammatory response depends on HIF factors.

- A Representation of the four upregulated k-means unsupervised clusters of upregulated genes in response to LPS in $CX_3CR1^{GFP/+}$ or $CX_3CR1^{GFP/+}; Sfrp1^{-/-}$ microglial cells. Eight different clusters were generated by Z-score covariation. The clusters are indicated in the heatmap of Fig 5F. Dotted lines indicate the mean variation of the genes included in each cluster.
- B Gene ontology enrichment analysis of different clusters and GO biological process annotated is represented by fold enrichment and colour-coded by adjusted *P*-value of enrichment by the hypergeometric test corrected for multiple comparisons by the Benjamini and Hochberg method, and number of genes of each cluster in that term.
- C Regulatory element analysis of different clusters. Specifically enriched transcription factors are represented by fold enrichment relative to the overall transcripts present in the microglia transcriptome. Coloured by log odds detection threshold by the hypergeometric test corrected for multiple comparisons by the Benjamini and Hochberg method, and the percentage of total targets for each transcription factor present in the cluster.

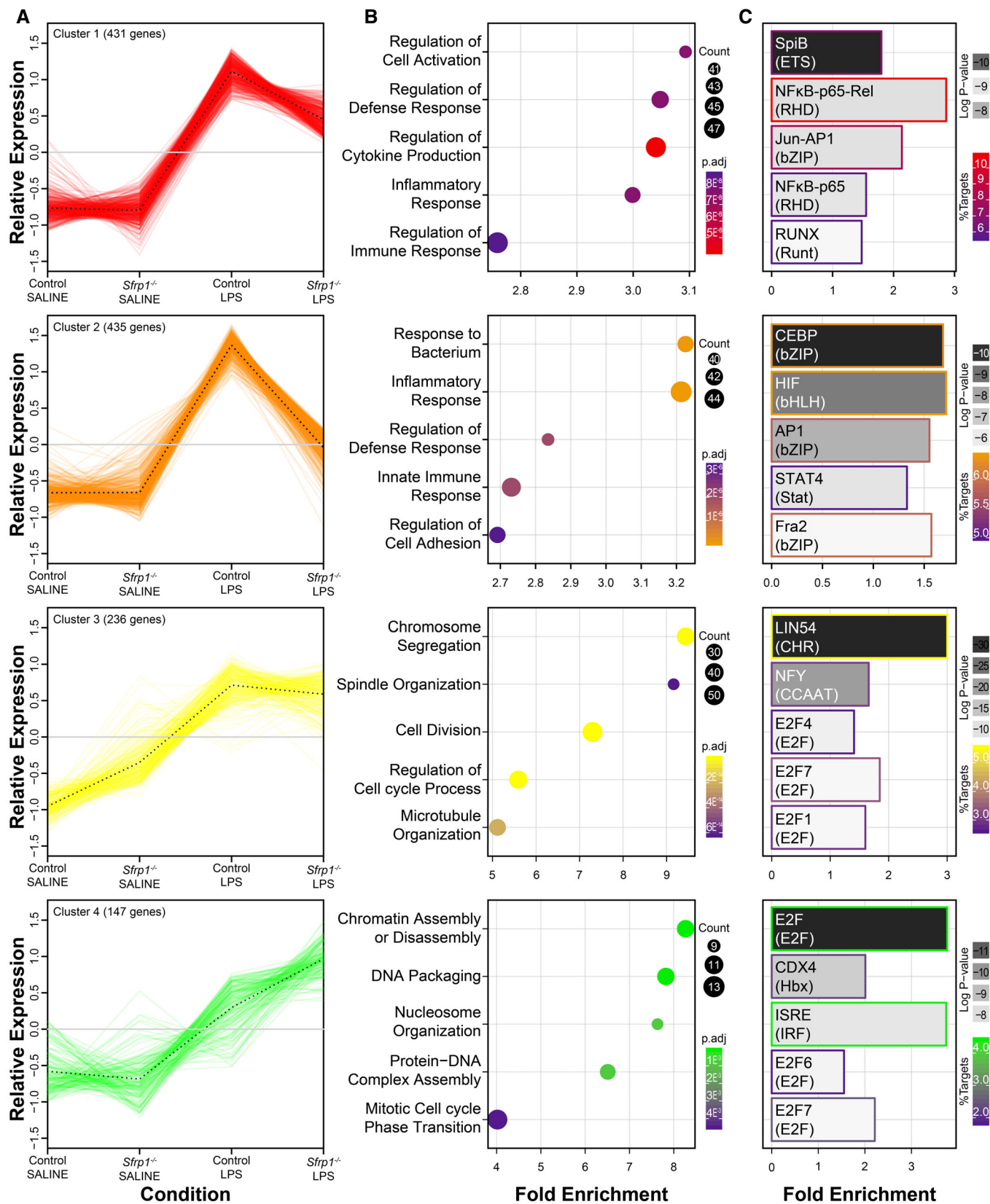


Figure EV4.